WING LIFT COEFFICIENT INCREMENT AT ZERO ANGLE OF ATTACK DUE TO DEPLOYMENT OF SINGLE-SLOTTED FLAPS AT LOW SPEEDS

1. NOTATION AND UNITS

		SI	*British*
A	aspect ratio, $2s/\bar{c}$		
a_1	basic wing lift-curve slope, $\mathrm{d}C_L/\mathrm{d}\alpha$ (see Item No. 70011)	rad^{-1}	rad^{-1}
$(a_1)_0$	basic aerofoil lift-curve slope in incompressible flow	rad^{-1}	rad^{-1}
C_L	lift coefficient; (lift per unit span)/qc for aerofoil, lift /qS for wing		
ΔC_{L0t}	increment in aerofoil lift coefficient at $\alpha = 0$ due to deployment of trailing-edge flap, based on c (see Item No. 94030)		
$\Delta C'_{L0t}$	increment in aerofoil lift coefficient at $\alpha = 0$ due to deployment of trailing-edge flap, based on c' (see Item No. 94030)		
ΔC_{L0tw}	increment in wing lift coefficient at $\alpha = 0$ due to deployment of trailing-edge flap, based on S		
$\Delta C'_{L1}$	increment in lift coefficient associated with deployment of single-slotted flap on aerofoil with lift-curve slope of 2π, based on c', Figure 2 (from Item No. 94030)		
c	chord of basic aerofoil chosen to be representative of wing, *i.e.* chord at mid-span of flap panel, see Sketch 1.1	m	ft
c'	extended aerofoil chord, *i.e.* chord with trailing-edge flap deployed, see Sketch 1.2	m	ft
c_r	wing root (centre-line) chord, see Sketch 1.1	m	ft
c_{t1}	chord of single-slotted trailing-edge flap, see Sketch 1.2	m	ft
Δc_{t1}	increment in c_{t1}, see Sketch 1.2	m	ft
c'_{t1}	extended chord of single-slotted trailing-edge flap, see Sketch 1.2	m	ft
$\bar{c}$	wing geometric mean chord	m	ft
$\bar{\bar{c}}$	wing aerodynamic mean chord	m	ft

Issued December 1993
With Amendment A, July 1995

J_{t1}	correlation factor (efficiency factor) for single-slotted trailing-edge flap, Figure 1 (from Item No. 94030)		
K_{f0}	flap-type correlation factor, see Section 4		
M	free-stream Mach number		
q	free-stream kinetic pressure	N/m^2	lbf/ft^2
$R_{\bar{\bar{c}}}$	Reynolds number based on free-stream conditions and $\bar{\bar{c}}$		
S	wing planform area, $2s\bar{c}$	m^2	ft^2
s	wing semi-span, see Sketch 1.1	m	ft
x	chordwise distance aft from aerofoil leading edge	m	ft
x_{ts}	chordwise location of flap-shroud trailing edge, see Sketch 1.2	m	ft
α	angle of attack (angle of incidence in Item No. 83040)	rad	rad
β	compressibility parameter, $(1-M^2)^{½}$		
δ°_{t1}	deflection of single-slotted trailing-edge flap, see Sketch 1.2	deg	deg
η	spanwise distance from wing centre-line as fraction of semi-span		
η_i	value of η at inboard limit of flap, see Sketch 1.1		
η_o	value of η at outboard limit of flap, see Sketch 1.1		
$\bar{\eta}$	value of η at spanwise centre of pressure for loading due to angle of attack, see Item No. 83040		
κ	wing taper parameter in Item No. 83040; $\int_0^1 (c/\bar{c})\eta \, d\eta$, giving $(1+2\lambda)/[3(1+\lambda)]$ for straight tapered wing		
Λ_h	flap hinge-line sweep angle, see Section 2 and Sketch 1.1	deg	deg
Λ_0	wing leading-edge sweep angle, see Sketch 1.1	deg	deg
$\Lambda_{¼}$	wing quarter-chord sweep angle, see Sketch 1.1	deg	deg
$\Lambda_{½}$	wing mid-chord sweep angle	deg	deg
Λ_1	wing trailing-edge sweep angle, see Sketch 1.1	deg	deg
λ	wing taper ratio (tip chord/root chord)		

Φ	part-span factor; lift coefficient increment due to part-span flaps extending symmetrically from wing centre-line divided by lift coefficient increment due to full-span flaps at same flap setting and wing angle of attack
Φ_i	value of Φ corresponding to η_i, Figure 3
Φ_o	value of Φ corresponding to η_o, Figure 3

Subscripts

full-span	denotes full-span flap ($\eta_i = 0$, $\eta_o = 1$)
part-span	denotes part-span flap ($\eta_i (\geq 0) < \eta_o \leq 1$)
$( )_{expt}$	denotes experimental value
$( )_{pred}$	denotes predicted value

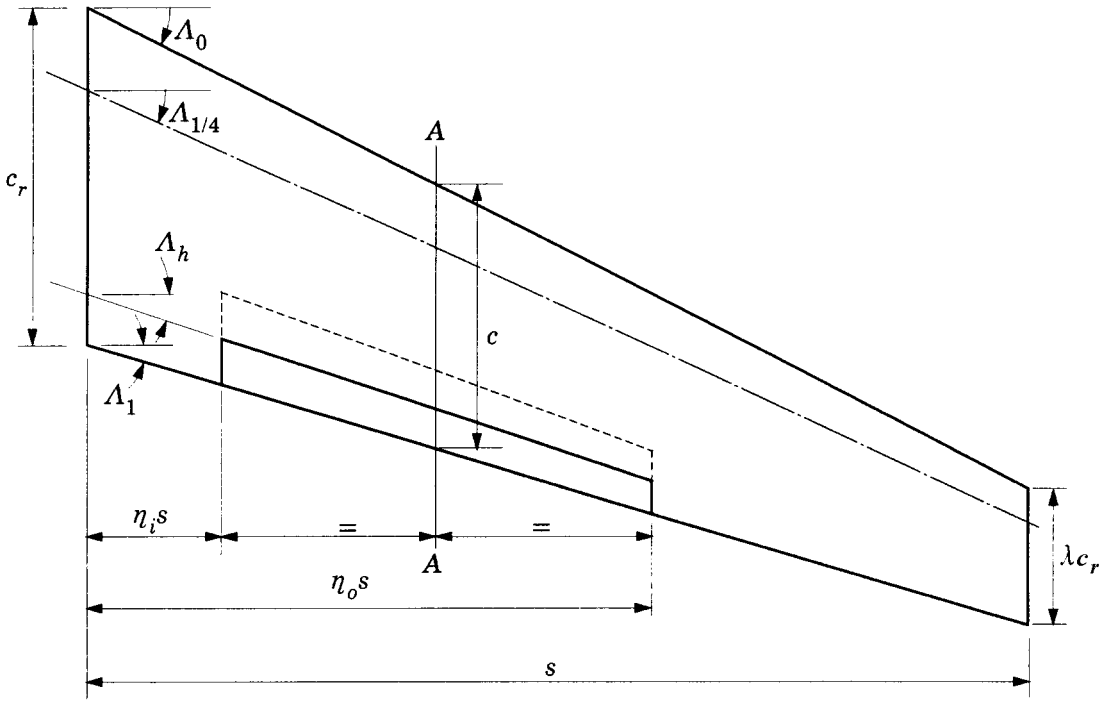

Sketch 1.1 Wing notation (flaps undeployed)

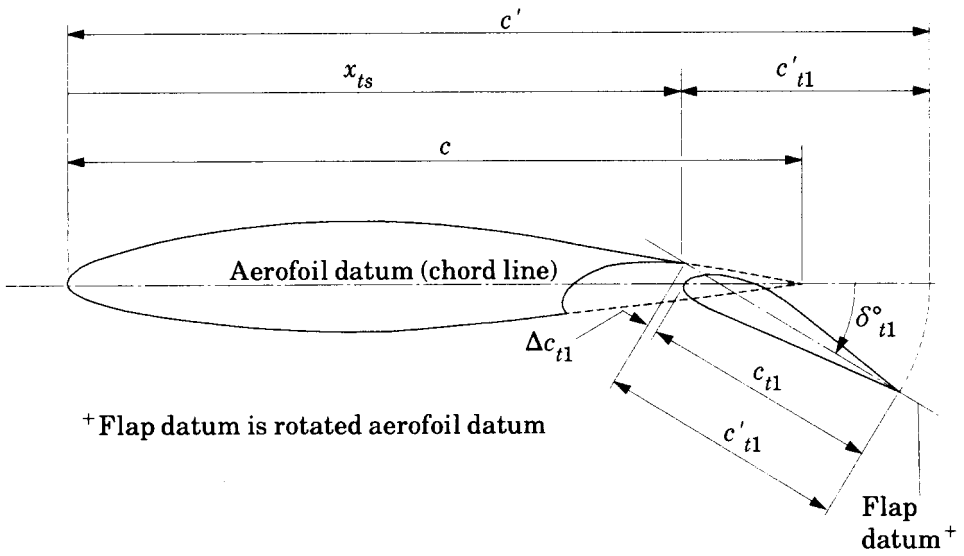

Sketch 1.2 Deployed single-slotted flap notation (at section AA in Sketch 1.1)

2. INTRODUCTION

In this Item the increment in lift coefficient at zero angle of attack due to the deployment of trailing-edge single-slotted flaps on a wing is derived from the increment in lift coefficient due to the deployment of a trailing-edge single-slotted flap on an aerofoil section that is representative of the wing. For wings with full-span flaps a factor dependent on planform geometry is applied to allow for three-dimensional effects. For wings with part-span flaps additional factors are introduced that are dependent on the flap and wing geometry. Finally, an empirical correlation factor, dependent on flap type, is applied. Wings with double-slotted or triple-slotted flaps are dealt with in Item No. 95021 (Reference 21).

At low speeds, the increment in lift coefficient at zero angle of attack, ΔC_{L0tw}, due to the deployment of a full-span flap on a high-aspect-ratio rectangular wing is strongly dependent on the corresponding value, ΔC_{L0t}, for an aerofoil/flap combination appropriate to the mid semi-span location. The main parameters that can influence ΔC_{L0t} are the flap angle, the aerofoil shape, the change of aerofoil chord length due to flap deployment, the effective chord of the flap, the flap type, and the flow Reynolds and Mach numbers. For flaps on wings the additional parameters that can influence ΔC_{L0tw} are the wing planform geometry (aspect ratio, taper ratio and sweep), the spanwise extent of the flap and flap hinge-line sweep angle. The effects of wing planform geometry are largely accounted for in terms of their effect on the wing lift-curve slope. Note that for a simple slotted flap or a Fowler flap it is normally sufficiently accurate to take the hinge-line sweep angle, Λ_h, to be either the sweep of the leading edge of the deployed flap or the sweep of the flap-shroud trailing edge, see Sketch 1.1.

3. REQUIRED DATA ITEMS

The ESDU Data Items that may be required in the use of this Item are:

Data Item No.[*]	*Derivation No.*	*To Determine*
70011	1	Wing lift-curve slope.
76003	2	Wing planform geometry.
83040	3	Wing spanwise centre of pressure location.
94030	4	ΔC_{L0t}.

[*] A Location Schedule is contained in the Organisational Guide-card Section of Volume 1a. This identifies the Volume in which each Item is held.

4. PREDICTION METHOD

Reports considered in the development of the method include work by Davison, Young and Lowry and Polhamus (References 16, 17 and 18) and Item No. 94030 (Derivation 4).

The resulting method uses Item No. 94030 for the characteristics of the representative aerofoil/flap combination coupled with empirical corrections for the effects of wing planform geometry, flap type and spanwise extent.

The aerofoil/flap combination that is taken as representative of the wing/flap system is that at the mid-span of the flap panel, see Sketch 1.1. By this means the effects of any spanwise variation of either the aerofoil section or the flap chord ratio are averaged out.

This Item contains a dedicated part-span factor that is dependent, in addition to flap spanwise extent, on the spanwise position of the centre of pressure of the loading due to angle of attack for the plain wing. It should be used in preference to the factor in Item No. 74012 (Reference 20) which was derived for plain flaps, since it gives an improved correlation of the slotted flap data. The results using the present method are consistent with those of the methods in References 18 and 19.

The method requires the use of streamwise flap angles and streamwise section and flap geometries, see Sketches 1.1 and 1.2. The primary effects of wing planform geometry in terms of aspect ratio, taper ratio and sweep are realised through their influence on the wing lift-curve slope. A flap-type correlation factor K_{f0} is required for single-slotted flaps.

The general expression for the increment in wing lift coefficient at zero angle of attack due to the deployment of a single-slotted trailing-edge flap on an aerofoil is

$$\Delta C_{L0t} = (c'/c)\Delta C'_{L0t} \tag{4.1}$$

where $\Delta C'_{L0t}$ is the increment in aerofoil lift coefficient at zero angle of attack based on the extended chord length c', and is given by Equation (4.1) of Item No. 94030, *viz*.

$$\Delta C'_{L0t} = J_{t1}\Delta C'_{L1}(a_1)_0/2\pi\,. \tag{4.2}$$

The general expression for the increment in wing lift coefficient at zero angle of attack due to the deployment

of a single-slotted trailing-edge flap is

$$\Delta C_{L0tw} = K_{f0}[\Delta C_{L0t}/(a_1)_0]a_1(\Phi_o - \Phi_i)\,, \tag{4.3}$$

which, with Equations (4.1) and (4.2), gives

$$\Delta C_{L0tw} = (c'/c)K_{f0}J_{t1}\Delta C'_{L1}(a_1/2\pi)(\Phi_o - \Phi_i)\,, \tag{4.4}$$

where

K_{f0}, the flap-type correlation factor, has been derived from the data of Derivations 5 to 7, 9 and 15 to be 1.05,

J_{t1} and $\Delta C'_{L1}$, given in Figures 1 and 2 respectively, have been reproduced from Item No. 94030,

a_1 is the wing lift-curve slope obtained from Item No. 70011 (Derivation 1)

and Φ_i and Φ_o, the part-span factors, are obtained from Figure 3 as functions of the inboard and outboard flap limits η_i and η_o respectively, and the spanwise centre of pressure position $\bar{\eta}$, which is obtained from Item No. 83040 (Derivation 3) for given values of βA, $A\tan\Lambda_{½}$ and the wing taper parameter κ.

5. EFFECTS OF MACH NUMBER AND REYNOLDS NUMBER

5.1 Mach Number Effects

High local Mach numbers will occur near the flap leading edge at low free-stream Mach numbers as a result of the deployment of a slotted flap. The significant effects of Mach number at free-stream Mach numbers greater than about 0.2 will depend on detailed section and slot geometry. None of the data considered for this Item was for a Mach number greater than 0.25.

5.2 Reynolds Number Effects

For the data used in the derivation of this Item no effect of Reynolds number on ΔC_{L0tw} was found. However, it should be noted that at very low Reynolds numbers ($R_{\bar{c}} < 0.6\times10^6$, say) the relatively thicker boundary layer reduces the effectiveness of the slot, thus reducing the increment in lift. If estimates are required for slotted flaps at such low Reynolds numbers, calculations for both plain flaps and slotted flaps will indicate the range of values within which ΔC_{L0tw} is likely to lie.

6. APPLICABILITY AND ACCURACY

6.1 Applicability

The method given in this Item for estimating the increment in lift coefficient at zero angle of attack due to the deployment of single-slotted trailing-edge flaps on a wing is directly applicable to straight-tapered wings covering a wide range of planform parameters. Table 6.1 summarises the parameter ranges that were used in developing the method. Note that the method should apply to the full range of flap chord ratios and deflection angles covered in Item No. 94030. It is known that the method does not apply to wings with greater sweep than those included in Table 6.1. A dependence on sweep is present in the method through its effect on a_1 and $\bar{\eta}$, but it was found that the correlation could not be improved by modelling separately an additional systematic effect of sweep.

TABLE 6.1

Parameter	*Range*
A	3.7 to 9
λ	0.2 to 1.0
Λ_0	0 to 48°
Λ_1	–12° to 39°
$^*\Lambda_h$	–8° to 41°
$A\tan\Lambda_0$	0 to 4.9
η_i	0 to 0.8
η_o	0.2 to 1.0
c_{t1}/c	0.2 to 0.34
$\delta°_{t1}$	10° to 45°
c'/c	1.0 to 1.34
$R_{\bar{c}} \times 10^{-6}$	0.6 to 4.4
M	≤ 0.25

* See Section 2 and Sketch 1.1.

For wings with cranked leading or trailing edges or curved tips it is suggested that the planform parameters needed to obtain a_1 and $\bar{\eta}$ be calculated for the equivalent straight-tapered planform as defined in Item No. 76003 (Derivation 2).

Although none of the wings involved in the wind-tunnel tests had more than one flap panel on each semi-span, the method can be applied to multiple panel cases by treating each panel separately and summing the contributions to obtain ΔC_{L0tw}.

6.2 Accuracy

Sketch 6.1 shows the comparison between predicted and experimental values of the increment in lift coefficient at zero angle of attack due to deployment of single-slotted flaps on unswept and swept wings. The experimental data were obtained from Derivations 5 to 15. The predicted and test data are correlated to within ±15 % for 90% of the data and to within ±10 % for 77% of the data.

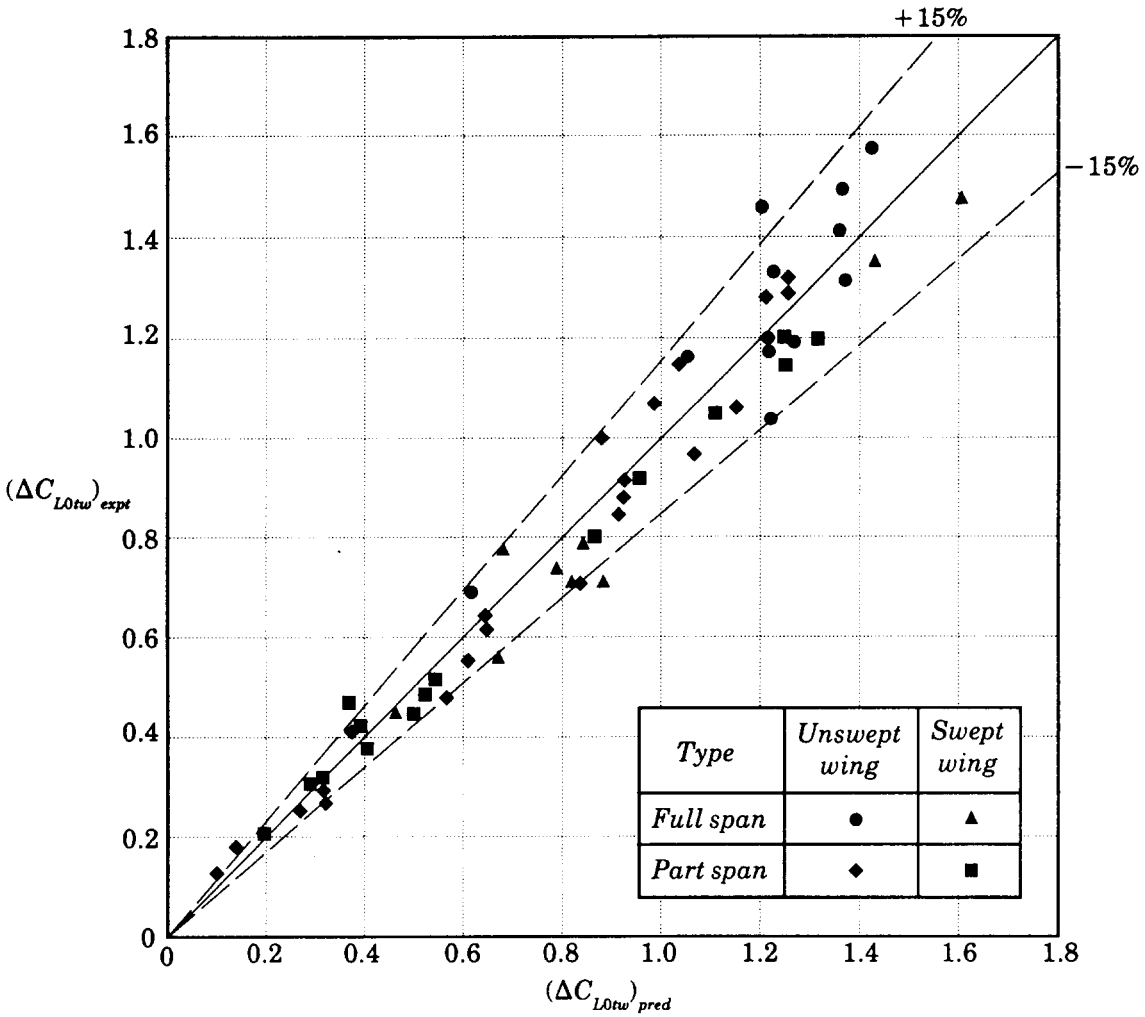

Sketch 6.1 Comparison of predicted and experimental values of ΔC_{L0tw}

Sketch 6.1 includes part-span cases. However, for those cases from Derivations 5, 6, 8 and 12, where experimental results are available for part-span and full-span flaps on the same wing, Sketch 6.2 shows the correlation of the predicted and experimental values of part-span to full-span lift coefficient increment ratio. The ratio is predicted to within ±10 % for 96% of the data, and to within ±5% for 80% of the data.

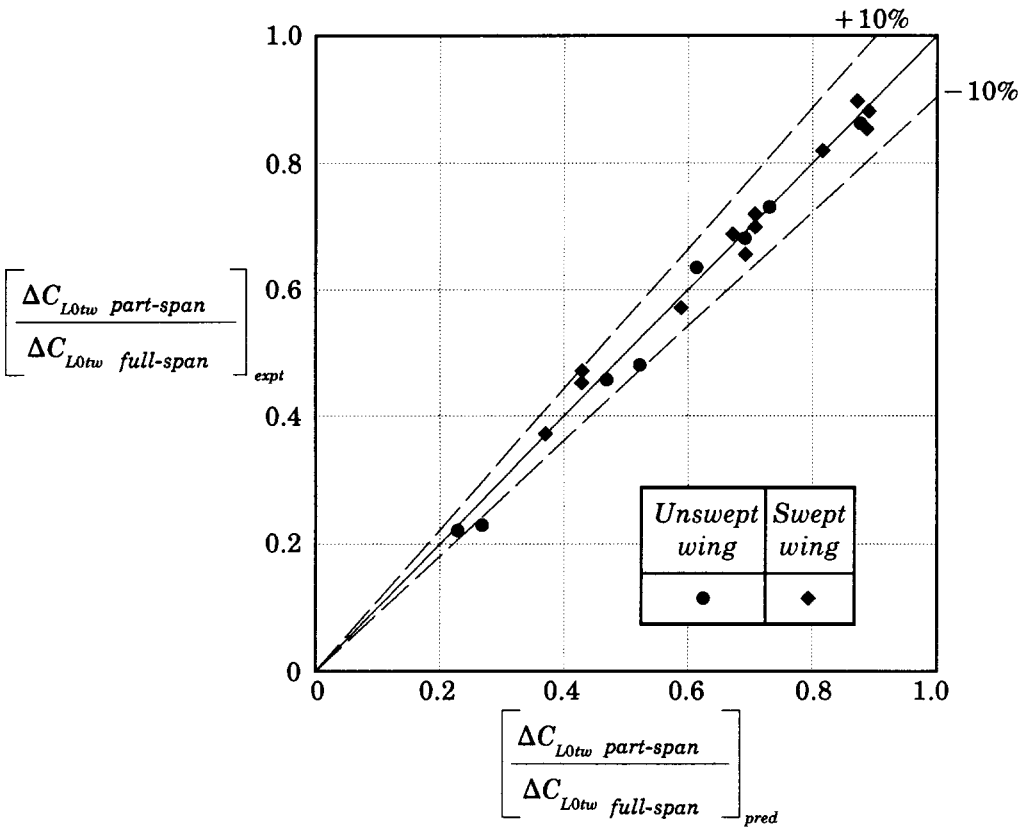

Sketch 6.2 Comparison of predicted and experimental values of part-span effects on ΔC_{L0tw}

7. DERIVATION AND REFERENCES

7.1 Derivation

The Derivation lists selected sources of information that have been used in the preparation of this Item.

7.1.1 ESDU Data Items

1. ESDU — Lift-curve slope and aerodynamic centre position of wings in inviscid subsonic flow.
ESDU International, Item No. 70011, 1970.
ESDUpac A7011.

2. ESDU — Geometric properties of cranked and straight tapered wing planforms.
ESDU International, Item No. 76003, 1976.

3. ESDU — Method for the rapid estimation of spanwise loading of wings with camber and twist in subsonic attached flow.
ESDU International, Item No. 83040, 1983.

4. ESDU — Increments in aerofoil lift coefficient at zero angle of attack and in maximum lift coefficient due to deployment of a single-slotted trailing-edge flap, with or without a leading-edge high-lift device, at low speeds.
ESDU International, Item No. 94030, 1995.

7.1.2 Wind-tunnel test reports

5. HOUSE, R.O. — The effects of partial span slotted flaps on the aerodynamic characteristics of a rectangular and a tapered NACA 23012 wing.
NACA tech. Note 719, 1939.

6. SIVELLS, J.C.
SPOONER, S.H. — Investigation in the Langley 19-foot pressure tunnel of two wings of NACA 65-210 and 64-210 airfoil sections with various type flaps.
NACA Report 942, 1947.

7. FISCHEL, J.
SCHNEITER, L.E. — High speed wind tunnel investigation of high lift and aileron control characteristics of a NACA 65-210 semi-span wing.
NACA tech. Note 1473, 1947.

8. SCHNEITER, L.E.
VOGLER, R.D. — Wind tunnel investigation at low speeds of various plug aileron and lift flap configurations on a 42° sweptback semi-span wing.
NACA RM L8K19 (TIL 2058), 1948.

9. FISCHEL, J.
VOGLER, R.D. — High lift and lateral control characteristics of a NACA 65_2-215 semi-span wing equipped with plug and retractable ailerons and a full span flap.
NACA tech. Note 1872, 1949.

10. HARPER, J.J. — Investigation at low speed of 45° and 60° sweptback, tapered, low drag wings equipped with various types of full-span trailing-edge flaps.
NACA tech. Note 2468, 1950.

11. NAESETH, R.L. — Low speed aerodynamic characteristics of a 45° sweptback wing with double slotted flaps. NACA RM L56A10 (TIL 5052), 1956.

12. LOVELL, D.A. — A wind tunnel investigation of the effects of flap span and deflection angle, wing planform and a body on the high lift performance of a 28° swept wing. RAE TR 76030, 1976.

13. PAULSON, J.W. — Wind-tunnel investigation of a Fowler flap and spoiler for an advanced general aviation wing. NASA tech. Note D-8236, 1976.

14. MORGAN, H.L. PAULSON, J.W. — Aerodynamic characteristics of wing-body configuration with two advanced general aviation airfoil sections and simple flap systems. NASA tech. Note D-8524, 1977.

15. APPLIN, Z.T. GENTRY, G.L. — Experimental and theoretical aerodynamic characteristics of a high lift semi-span model. NASA tech. Paper 2990, 1990.

7.2 References

The References given are sources of information supplementary to that given in this Item.

16. DAVISON, F.J. — A method for estimating the aerodynamic characteristics of flaps. Saunders Roe Ltd. Aerodynamics Dept, c.1950.

17. YOUNG, A.D. — The aerodynamic characteristics of flaps. RAE Report No. Aero 2185, 1947. ARC R&M 2622, 1953.

18. LOWRY, J.G. POLHAMUS, E.C. — A method for predicting lift increments due to flap deflection at low angles of attack in incompressible flow. NACA tech. Note 3911, 1957.

19. McKIE, J. — The estimation of the loading on swept wings with extending chord flaps at subsonic speeds. RAE TR 69034, 1969.

20. ESDU — Conversion of lift coefficient increment due to flaps from full span to part span. ESDU International, Item No. 74012, 1974.

21. ESDU — Wing lift coefficient increment at zero angle of attack due to deployment of double-slotted or triple-slotted flaps at low speeds. ESDU International, Item No. 95021, 1995.

8. EXAMPLE

Estimate the increment in lift coefficient at zero angle of attack at a Mach number $M = 0.2$ for the wing with a part-span single-slotted trailing-edge flap shown in Sketch 8.1. The wing has the planform parameter values

$$A = 8\,,\ \Lambda_{1/4} = 25°\ \text{and}\ \lambda = 0.4\,.$$

The flap extends from the wing centre-line to 60% of the semi-span. The location of the flap-shroud trailing edge and the flap chord are each a constant fraction of the local wing chord. The required streamwise geometrical parameters for the flap are

$$x_{ts}/c = 0.85\,,\quad c_{t1}/c = 0.30\,,\quad \Delta c_{t1}/c = -0.02\,,\quad \delta°_{t1} = 30°\,.$$

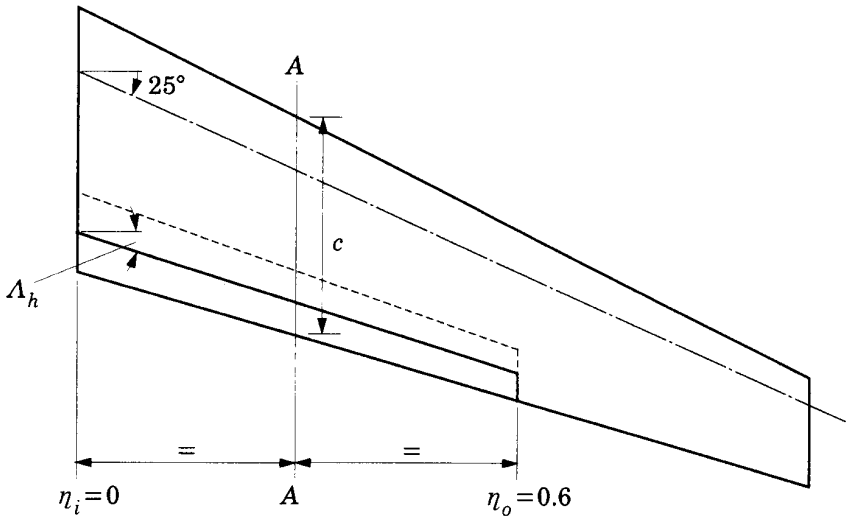

Wing planform (flap undeployed)

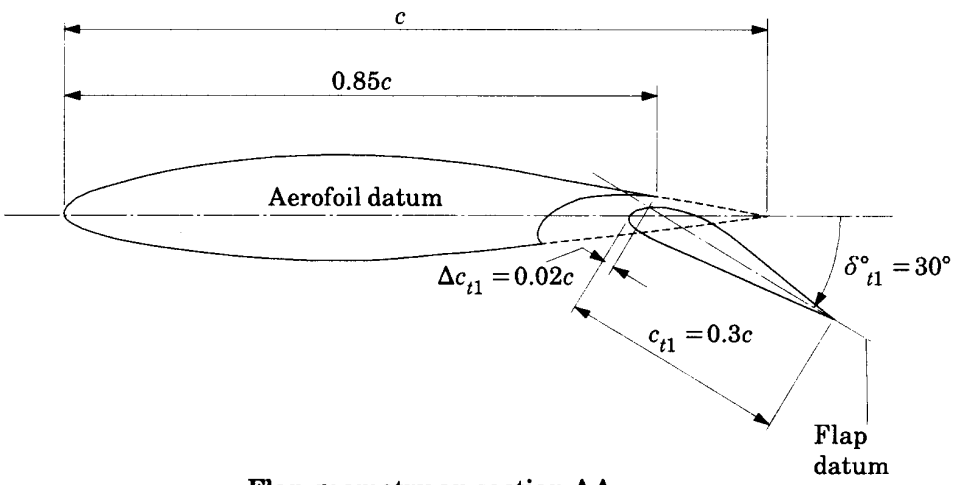

Flap geometry on section AA

Sketch 8.1

1. Check that the sweep angles are within the range of applicability of the method

From the relationships for planform geometry given in Item No. 76003,

$$\Lambda_0 = \tan^{-1}\left[\tan\Lambda_{¼} + \frac{1}{A}\left(\frac{1-\lambda}{1+\lambda}\right)\right]$$

$$= \tan^{-1}\left[\tan 25° + \frac{1}{8}\left(\frac{1-0.4}{1+0.4}\right)\right]$$

$$= 27.5° .$$

$$\Lambda_1 = \tan^{-1}\left[\tan\Lambda_{¼} - \frac{3}{A}\left(\frac{1-\lambda}{1+\lambda}\right)\right]$$

$$= \tan^{-1}\left[\tan 25° - \frac{3}{8}\left(\frac{1-0.4}{1+0.4}\right)\right]$$

$$= 17.0°$$

The hinge-line sweep angle, Λ_h, taken as the sweep angle of the flap-shroud trailing edge at $x_{ts} = 0.85c$, is given by

$$\Lambda_h = \tan^{-1}\left[\tan\Lambda_{¼} + \frac{4}{A}\left(\frac{1}{4} - 0.85\right)\left(\frac{1-\lambda}{1+\lambda}\right)\right]$$

$$= 18.7° .$$

From Table 6.1 it is seen that the values of Λ_0, Λ_1 and Λ_h all lie within the permitted ranges.

2. Determine the required wing planform parameters

From the relationship in Item No. 76003, with the given values of A, $\Lambda_{¼}$ and λ

$$A\tan\Lambda_{½} = A\tan\Lambda_{¼} - \frac{1-\lambda}{1+\lambda}$$

$$= 8\times \tan 25° - \frac{1-0.4}{1+0.4}$$

$$= 3.302.$$

The wing taper parameter κ is given by

$$\kappa = \frac{1+2\lambda}{3(1+\lambda)}$$

$$= \frac{1+2\times 0.4}{3(1+0.4)}$$

$$= 0.429.$$

3. Determine $\bar{\eta}$ from Item No. 83040

Since $M = 0.2$,

$$\beta A = (1-M^2)^{½}A$$

$$= (1-0.2^2)^{½}\times 8$$

$$= 7.84,$$

and so with $A\tan\Lambda_{½} = 3.302$ and $\kappa = 0.429$ a cross-plot in βA using Figures 1 to 5 of Item No. 83040 gives

$$\bar{\eta} = 0.437.$$

4. Determine a_1 from Item No. 70011

With $A\tan\Lambda_{½} = 3.302$ and $\beta A = 7.84$, a cross-plot in λ from Figures 1a to 1e of Item No. 70011, for $\lambda = 0.4$ gives

$$\frac{1}{A}\frac{dC_L}{d\alpha} = 0.571 \text{ rad}^{-1}.$$

Hence

$$a_1 = \frac{dC_L}{d\alpha} = \frac{1}{A}\frac{dC_L}{d\alpha}\times A$$

$$= 0.571 \times 8$$

$$= 4.57 \text{ rad}^{-1}.$$

5. Obtain c'_{t1}/c' and c'/c

From the definitions in Sketch 1.2, the dimensions of Sketch 8.1 give

$$c'_{t1}/c = c_{t1}/c + \Delta c_{t1}/c$$
$$= 0.30 - 0.02$$
$$= 0.28$$
$$\text{and } c'/c = x_{ts}/c + c'_{t1}/c$$
$$= 0.85 + 0.28$$
$$= 1.13 ,$$

so that

$$c'_{t1}/c' = (c'_{t1}/c)/(c'/c)$$
$$= 0.28/1.13$$
$$= 0.248 .$$

6. Determine ΔC_{L0tw}

From Equation (4.4)

$$\Delta C_{L0tw} = (c'/c)K_{f0}J_{t1}\Delta C'_{L1}(a_1/2\pi)(\Phi_o - \Phi_i) ,$$

in which

$$K_{f0} = 1.05 .$$

Figure 1 with $\delta^\circ_{t1} = 30^\circ$, gives

$$J_{t1} = 1.17$$

and Figure 2 with $\delta^\circ_{t1} = 30^\circ$, $c'_{t1}/c' = 0.248$, gives

$$\Delta C'_{L1} = 1.221 .$$

From Figure 3, for $\eta_o = 0.6$ and $\bar{\eta} = 0.437$

$$\Phi_o = 0.70$$

and, for $\eta_i = 0$

$$\Phi_i = 0 .$$

Therefore,

$$\Delta C_{L0tw} = 1.13 \times 1.05 \times 1.17 \times 1.221 \times (4.75/2\pi) \times (0.70 - 0)$$

$$= 0.863 \approx 0.86 .$$

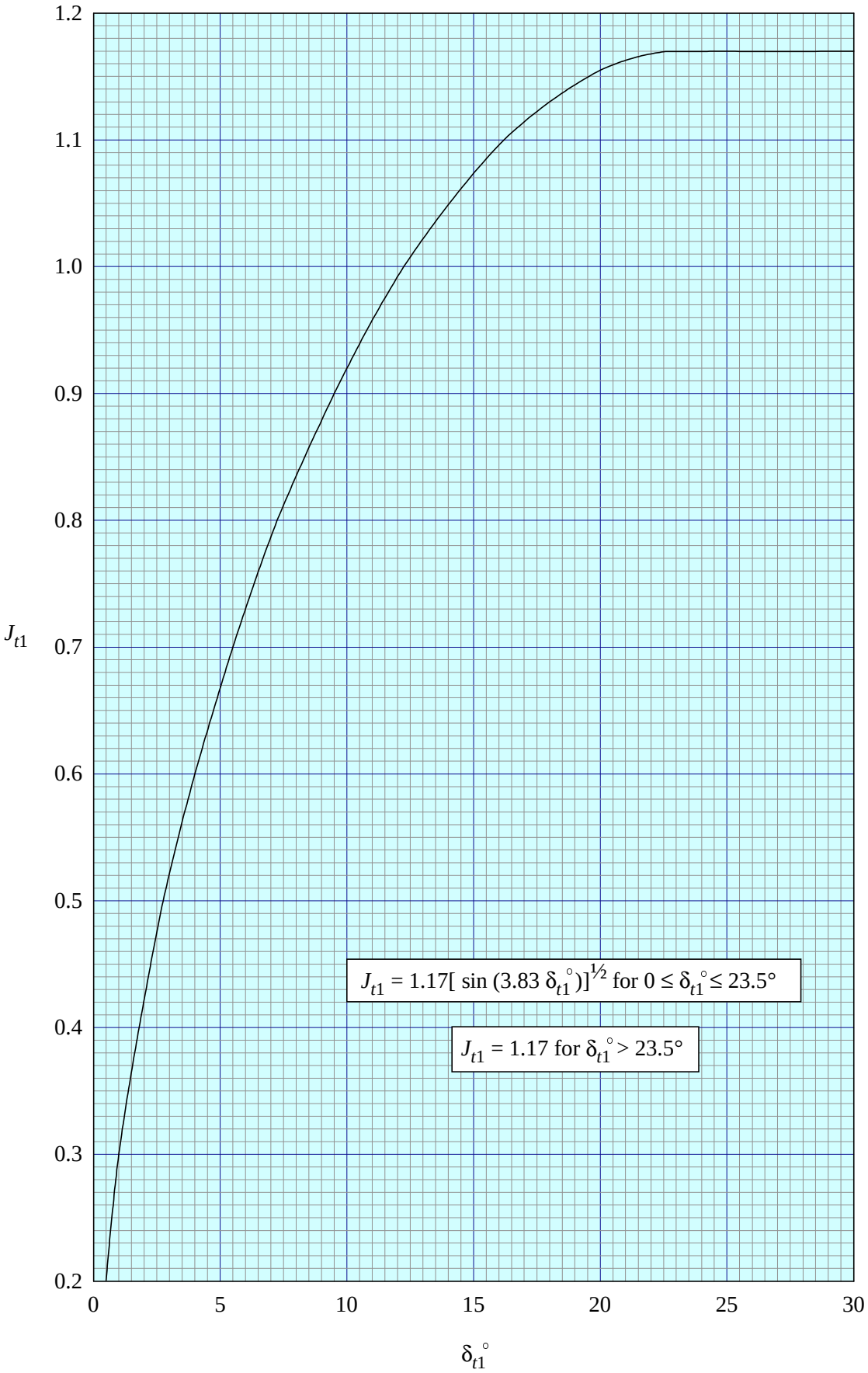
1.2
1.1
1.0
0.9
0.8
0.7
0.6
0.5
0.4
0.3
0.2
J_{t1}
0
5
10
15
20
25
30
δ_{t1}°
$J_{t1} = 1.17[\sin(3.83\,\delta_{t1}^{\circ})]^{1/2}$ for $0 \le \delta_{t1}^{\circ} \le 23.5°$
$J_{t1} = 1.17$ for $\delta_{t1}^{\circ} > 23.5°$

FIGURE 1

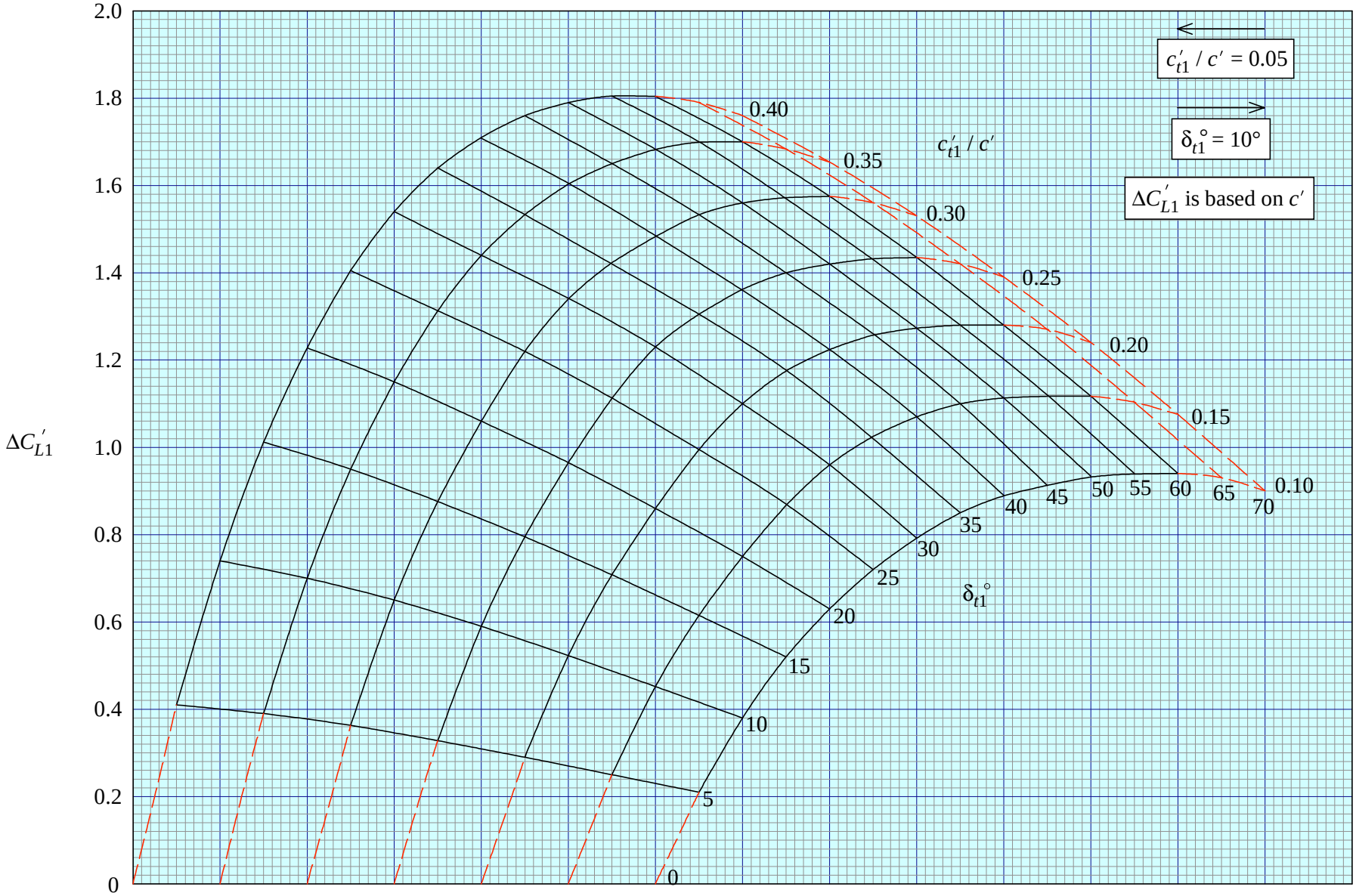
2.0
1.8
1.6
1.4
1.2
1.0
0.8
0.6
0.4
0.2
0
$\Delta C_{L1}'$
c_{t1}' / c'
0.40
0.35
0.30
0.25
0.20
0.15
0.10
$c_{t1}' / c' = 0.05$
$\delta_{t1}° = 10°$
$\Delta C_{L1}'$ is based on c'
$\delta_{t1}°$
0
5
10
15
20
25
30
35
40
45
50
55
60
65
70

FIGURE 2

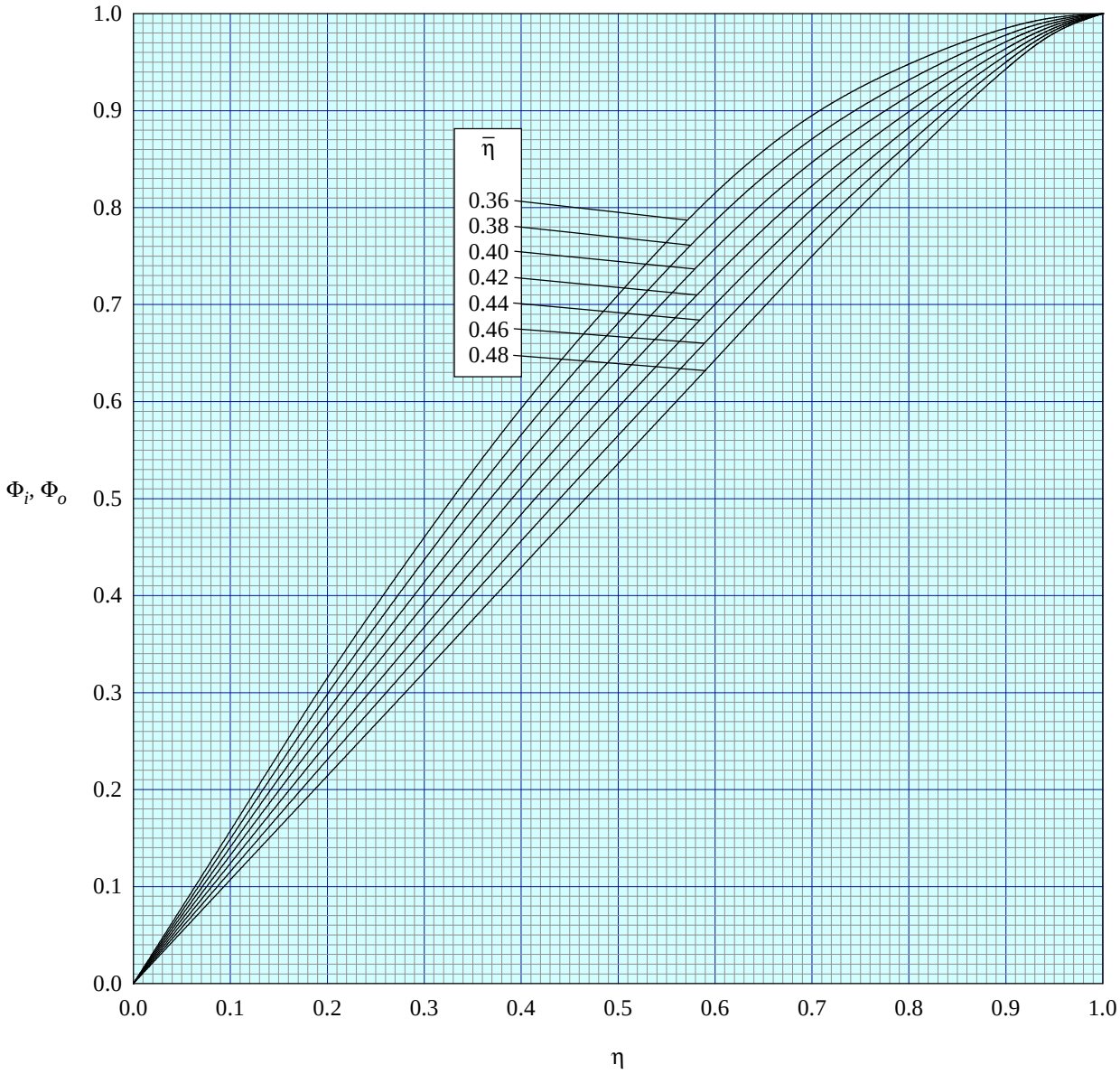
1.0
0.9
0.8
0.7
0.6
0.5
0.4
0.3
0.2
0.1
0.0
Φi, Φo
η̄
0.36
0.38
0.40
0.42
0.44
0.46
0.48
0.0
0.1
0.2
0.3
0.4
0.5
0.6
0.7
0.8
0.9
1.0
η

FIGURE 3

THE PREPARATION OF THIS DATA ITEM

The work on this particular Item, which supersedes Item No. Aero F.01.01.08, was monitored and guided by the Aerodynamics Committee which first met in 1942 and now has the following membership:

Chairman

Mr H.C. Garner	–	Independent

Members

Mr G.E. Bean*	–	Boeing Commercial Airplane Co., Seattle, Wash., USA
Dr N.T. Birch	–	Rolls-Royce plc, Derby
Dr P.C. Dexter	–	British Aerospace plc, Sowerby Research Centre, Bristol
Mr J.R.J. Dovey	–	Independent
Dr K.P. Garry	–	Cranfield University
Mr D. Graham*	–	Northrop Grumman Corp., Pico Rivera, Calif., USA
Mr M.J. Green	–	Avro International Aerospace Ltd, Woodford
Dr H.P. Horton	–	Queen Mary and Westfield College, University of London
Dr D.W. Hurst	–	University of Southampton
Mr P.K. Jones	–	Independent
Mr K. Karling*	–	Saab-Scania AB, Linköping, Sweden
Mr M. Maurel	–	Aérospatiale, Toulouse, France
Mr C.M. Newbold	–	Aircraft Research Association, Bedford
Mr J.B. Newton	–	British Aerospace Defence Ltd, Warton
Mr R. Sanderson	–	Daimler-Benz Aerospace Airbus GmbH, Bremen, Germany
Mr A.E. Sewell*	–	McDonnell Douglas Corp., Long Beach, Calif., USA
Mr M.R. Smith	–	British Aerospace Airbus Ltd, Bristol
Mr J. Tweedie	–	Short Brothers plc, Belfast.

* Corresponding Member

The technical work in the assessment of the available information and the construction and subsequent development of the Data Item was carried out under contract to ESDU by Mr J.R.J. Dovey.